Inorganic Chemistry

Article

pubs.acs.org/IC

Synthesis and Characterization of Heterobimetallic Complexes with Direct Cu−M Bonds (M = Cr, Mn, Co, Mo, Ru, W) Supported by *N*-Heterocyclic Carbene Ligands: A Toolkit for Catalytic Reaction Discovery

Suparna Banerjee,[†] Malkanthi K. Karunananda,[†] Sharareh Bagherzadeh, Upul Jayarathne, Sean R. Parmelee, Greyson W. Waldhart, and Neal P. Mankad*

Department of Chemistry, University of Illinois at Chicago, 845 West Taylor Street, Chicago, Illinois 60607, United States

Supporting Information

ABSTRACT: Building upon the precedent of catalytically active (NHC)Cu−FeCp-$(CO)_2$ complexes, a series of (NHC)Cu−[M] complexes were synthesized via the addition of $Na^+[M]^-$ reagents to (NHC)CuCl synthons. The different $[M]^-$ anions used span a range of 7×10^7 relative nucleophilicity units, allowing for controlled variation of nucleophile/electrophile pairing in the heterobimetallic species. Direct Cu−M bonds (M = Cr, Mn, Co, Mo, Ru, W) formed readily when the bulky IPr carbene was used as a support. Crystallographic characterization and computational examination of these complexes was conducted. For the smaller IMes carbene, structural isomerism was observed when using the weakest $[M]^-$ nucleophiles, with (IMes)Cu−[M] and $\{(IMes)_2Cu\}\{Cu[M]_2\}$ isomers being observed in equilibrium. Collectively, the series of complexes provides a toolbox for catalytic reaction discovery with precise control of structure−function relationships.

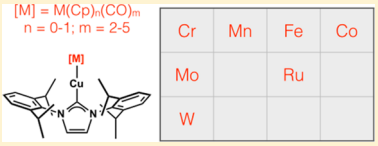

INTRODUCTION

The field of organometallics has predominantly focused on reaction chemistry at single metal sites, and certain metals (e.g., Rh, Pd, Ir, Pt) have emerged as the privileged choices for conducting fundamental reaction steps (e.g., oxidative addition, reductive elimination) necessary in homogeneous catalysis. Analogous chemistry at bimetallic reaction centers can allow for new modes of reactivity and/or selectivity to emerge with these privileged metals[1] and, additionally, can expand the scope of these fundamental reaction motifs to include nontraditional chemical elements that may be desirable as alternatives.[2] Applications in homogeneous catalysis for systems that exploit such metal−metal cooperativity continue to emerge.[3]

Our research group recently began studying heterobimetallic complexes featuring direct Cu−Fe and Zn−Fe bonds constructed through the addition of $[Fp]^-$ to Cu- and Zn-electrophiles supported by *N*-heterocyclic carbene (NHC) ligands.[4] Not only are these complexes capable of facilitating interesting small molecule activation reactions,[5] but one of these complexes, (IPr)Cu−Fp (where IPr = *N*,*N*′-bis(2,6-diisopropylphenyl)imidazol-2-ylidene; Fp = $FeCp(CO)_2$), was found to be the first nonprecious metal catalyst for the direct C−H borylation of arenes.[6,7] The unique reactivity of this complex is, in part, enabled by the special ability of NHCs to stabilize reactive catalytic intermediates featuring Cu.[8] The proposed mechanism for this bimetallic C−H borylation reaction involves bimetallic analogues of the classical oxidative addition and reductive elimination reactions, and so we have speculated that other reactions traditionally conducted with single-site noble-metal catalysts might be viable using this bimetallic approach.[9] In order to probe such questions and fully explore the possibilities of such heterobimetallic catalysts, it is first necessary to synthesize and characterize a more-complete range of (NHC)Cu−[M] complexes that can collectively access a vast chemical reactivity space.[10]

The mechanism for the bimetallic C−H borylation reaction relies on subtle interplay between the nucleophilicity of the $[Fp]^-$ fragment and the electrophilicity of the $[(IPr)Cu]^+$ fragment and highlights the need to vary both of these parameters in a controlled manner for future reaction development. Fortunately, $[Fp]^-$ is but one of a series of anionic metal carbonyls whose relative nucleophilicities have been quantified and span an impressively large range (Figure 1).[11] These nucleophilicity data, which represent a kinetic parameter, also correlate well with thermodynamic reduction potentials.[12] Using this series of nucleophiles, here, we report the synthesis and crystallographic characterization of an expanded set of (NHC)Cu−[M] complexes, examine the nature of the metal−metal bonds computationally, and highlight subtle effects of NHC variation on structural isomerism in these complexes. Collectively, this series of complexes provides a toolbox of potential catalysts for future reaction discovery, with fine control of structure−function relationships, that will access an expansive chemical space unavailable to just the initial (NHC)Cu−Fp complexes.

RESULTS AND DISCUSSION

Synthesis and Characterization of IPr Complexes. Akin to our previously reported synthesis of (IPr)Cu−Fp,[4] the

Received: August 13, 2014
Published: October 2, 2014

   dx.doi.org/10.1021/ic5019778 | Inorg. Chem. 2014, 53, 11307−11315

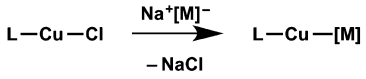

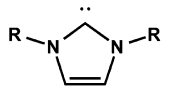

L = IPr (R = dipp) or IMes (R = mes)

[M]−	Relative Nucleophilicity
$FeCp(CO)_2^-$ (Fp^-)	70,000,000
$RuCp(CO)_2^-$ (Rp^-)	7,500,000
$WCp(CO)_3^-$ (Wp^-)	500
$Mn(CO)_5^-$ (Mc^-)	77
$MoCp(CO)_3^-$ (Mp^-)	67
$CrCp(CO)_3^-$ (Crp^-)	4
$Co(CO)_4^-$ (Cc^-)	1

Figure 1. Synthesis of (NHC)Cu−[M] complexes. Abbreviations and relative nucleophilicity data for the different $[M]^-$ anions used in this study have been taken from ref 11. [Legend: dipp = 2,6-diisopropylphenyl, mes = 2,4,6-trimethylphenyl.]

complexes (IPr)Cu−Rp and (IPr)Cu−Wp were readily prepared in yields of 73% and 91%, respectively, from 1:1 mixtures of (IPr)CuCl and the appropriate Na[M] reagent at room temperature (see Figure 1 for abbreviation definitions). Analogous conditions did not provide quantitative conversion to products for weaker nucleophiles on a reasonable time scale, and so more forcing conditions were deemed necessary. For example, (IPr)Cu−Cc was prepared in 83% yield from a 1.2:1 mixture of Na^+Cc^- and (IPr)CuCl at 36 °C, while (IPr)Cu−Crp and (IPr)Cu−Mc were prepared in yields of 78% and 85%, respectively, from 3:1 mixtures. The complex (IPr)Cu−Mp has been synthesized previously both by the salt metathesis method used here[4] and by protonolysis of (IPr)CuOH by HMp.[13] The Cp-containing complexes all were yellow in color, while the complexes lacking Cp groups were colorless in crystalline form. These new complexes add to the somewhat limited set of bimetallic complexes featuring direct Cu−M bonds for M = Ru,[14] W,[15] Mn,[16] Cr,[15c,17] and Co.[18]

All of the new complexes were characterized by nuclear magnetic resonance (^{1}H NMR and $^{13}C\{^1H\}$ NMR), solid-state Fourier transform infrared (FT-IR) spectroscopy, and combustion analysis. In all cases, the NMR spectra were consistent with a single IPr environment, implying free Cu−M bond rotation at room temperature on the NMR time scale.[19] The infrared (IR)-active vibrations corresponding to CO ligands within the anionic [M] fragments were all within the terminal CO regions of the spectra, precluding the possibility of classical bridging CO ligands in any of the complexes. The CO vibrational frequencies tended to increase going down the Group 8 column but decrease going down the Group 6 column (i.e., ν_{CO}: Fe < Ru, Cr ≈ Mo > W). Similar trends are observed for the anionic $[M]^-$ monometallics (see Table 1), indicating that the presence of a Cu−M bond perturbs M−CO bonding consistently across the series. The complexes in the (IPr)Cu−[M] series all were found to be air-sensitive but stable for multiple weeks at room temperature under inert atmospheres.

Solid-state structures of the Ru, Mn, Cr, and Co derivatives determined by single-crystal X-ray diffraction (XRD) are depicted in Figure 2. Two independent molecules with different

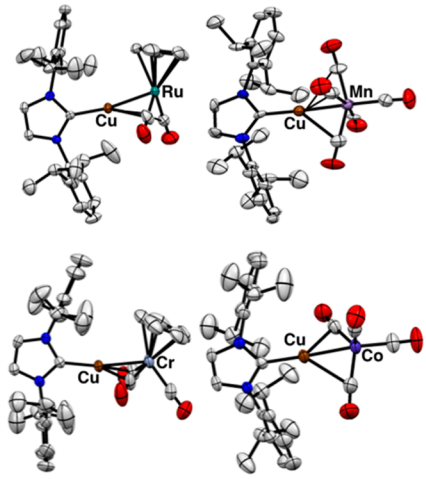

Figure 2. Solid-state structures of (IPr)Cu−Rp, (IPr)Cu−Mc, (IPr)Cu−Crp, and (IPr)Cu−Cc as 50% probability thermal ellipsoids. Hydrogen atoms and co-crystallized solvent molecules have been omitted.

structures were located in the asymmetric unit for (IPr)Cu−Wp (Figure 3a). One molecule featured a linear Cu−W−Cp(centroid) angle (175.60°) and comparatively shorter Cu−W distance (2.5345(6) Å). The second molecule was isostructural to the Cr and Mo derivatives, featuring a bent Cu−W−Cp(centroid) angle (119.81°) and a slightly longer Cu−W distance (2.5599(6) Å). Key structural parameters for the entire series of complexes are given in Table 1.

The Cu−M distances can be compared using Cotton's formal shortness ratio (FSR) calculations to correct for metal sizes (Table 1).[22,23] As expected, FSR values for the metal−metal single bonds were all near 1. Periodic trends in FSR were not immediately evident: for example, FSR decreased going down the Group 6 triad but increased going down Group 8. However, a clear trend emerged by which FSR increased with

Table 1. Key Bond Distances and Vibrational Data for (IPr)Cu−[M] Complexes

complex[a]	d(Cu−M) (Å)/FSR[b]	d(Cu···CO) (Å)[c]	ν_{CO} of (IPr)Cu−[M] (cm^{-1})	ν_{CO} of $[M]^-$ (cm^{-1})
(IPr)Cu−Fp[d]	2.3462(5)/1.004	*2.423(3), 2.749(3)*	1914, 1849	1854, 1775[i]
(IPr)Cu−Rp	2.4387(9)/1.010	*2.610(6), 2.828(5)*	1940, 1867	1895, 1812[j]
(IPr)Cu−Wp[e]	2.5345(6)/1.025	*2.272(5), 2.300(7), 2.468(6)*	1920, 1818, 1784	1896, 1786, 1746[h]
(IPr)Cu−Wp[f]	2.5599(6)/1.035	*2.294(7), 2.280(5)*, 3.858(6)		
(IPr)Cu−Mc	2.415(1)/1.032	*2.63(1), 2.66(1), 2.644(6)*, 2.973(6)	2042, 1885, 1830	1896, 1862, 1830[h]
(IPr)Cu−Mp[g]	2.5600(8)/1.039	*2.193(7), 2.322(7)*, 3.861(7)	1926, 1822, 1799	1898, 1790, 1750[h]
(IPr)Cu−Crp	2.4569(7)/1.048	*2.174(4), 2.237(5)*, 3.547(5)	1914, 1822, 1792	1900, 1800, 1752[h]
(IPr)Cu−Cc	2.3423(6)/1.005	*2.354(4), 2.444(4)*, 2.933(4), 4.077(4)	2038, 1957, 1915	1890, 1857[h]

[a]Decreasing order of $[M]^-$ nucleophilicity; see ref 11. [b]Formal shortness ratio; see ref 22. [c]Only distances within van der Waals contact (<4.2 Å)[24] are listed. Italicized values represent semibridging carbonyls ($0.1 < \alpha < 0.6$), and nonitalicized values represent terminal carbonyls ($\alpha \geq 0.6$); see ref 25. [d]Data taken from ref 4. [e]Data for the first of two independent molecules found in the asymmetric unit. [f]Data for the second of two independent molecules found in the asymmetric unit. [g]Data taken from ref 13. [h]Data taken from ref 20. [i]Data taken from ref 4b. [j]Data taken from ref 21.

dx.doi.org/10.1021/ic5019778 | Inorg. Chem. 2014, 53, 11307−11315

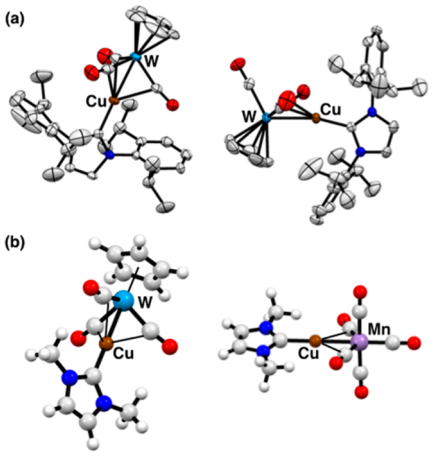

Figure 3. (a) Two independent (IPr)Cu–Wp molecules found in the same asymmetric unit, depicted as 50% probability thermal ellipsoids. Hydrogen atoms and co-crystallized solvent molecules have been omitted. (b) Optimized structures of (IMe)Cu–Wp and (IMe)Cu–Mc determined by density functional theory (DFT) energy minimization (BVP86/LANL2TZ(f)/6-311+G(d)).

decreasing nucleophilicity of $[M]^-$, indicating that stronger nucleophiles result in shorter Cu–M bonds. An outlier in this regard was (IPr)Cu–Cc, which exhibited an anamolously short Cu–Co FSR value, despite the weakly nucleophilic character of $[Cc]^-$.

All of the CO ligands in the (IPr)Cu–[M] series exhibited linear geometries at carbon: $169.2(5)° \leq \angle(M–C–O) \leq 178.4(3)°$. This observation in combination with FT-IR spectroscopy (*vide supra*) eliminated the possibility of any bridging CO ligands being present. However, all of the complexes in the series featured multiple CO ligands within van der Waals contact range of the Cu centers,[24] in agreement with our previous observation of close Cu···CO contacts in the solid state for the Fe and Mo derivatives.[4] Furthermore, nonclassical bridging interactions were evident upon cursory examination of the local geometries at the Mn and Co centers, which deviate significantly from idealized octahedral and trigonal bipyramidal geometries, respectively (see Figure 2), because of 2–3 CO ligands per molecule "leaning" toward the Cu centers. The asymmetry parameter (α) was used to determine the presence of so-called "semi-bridging" CO ligands ($0.1 < \alpha < 0.6$).[25] Using this analysis, two semibridging CO ligands were detected per solid-state structure in the Fe, Ru, Mo, Cr, and Co derivatives (Figure 2), as well as in one of the two W structures (Figure 3a).[26] The other W structure (Figure 3a), as well as the Mn structure (Figure 2), featured three semibridging CO ligands each. The Cu···CO distances for the semibridging interactions span the range $2.174(4)\ \text{Å} \leq d(\text{Cu}\cdots\text{CO}) \leq 2.828(5)\ \text{Å}$, while the shortest Cu···CO distance for a terminal CO ligand ($\alpha \geq 0.6$)[25] was 2.973(6) Å (in the Mn derivative). The presence of two independent structures for (IPr)Cu–Wp in the same asymmetric unit, each with a different number of semibridging CO ligands, highlights the weak nature of these interactions in comparison to crystal packing forces.

Computational Analysis. We have previously established, through computational methods[4] as well as chemical reactivity studies[4–6] and spectroscopic analyses,[4b] that the Cu–Fe bond in (IPr)Cu–Fp is polarized such that the Cu retains positively charged, electrophilic character and the Fe retains negatively charged, nucleophilic character (i.e., the Cu–Fe bond possesses a significant degree of ionic character). Because of the varying nucleophilicities and reducing potentials of the $[M]^-$ anions used in this study to construct (IPr)Cu–[M] complexes,[11,12] we chose to undertake computational analysis to examine how this polar, ionic Cu–M bonding is affected by the identity of $[M]^-$.

Model complexes featuring the truncated IMe ligand (where IMe = *N*,*N*′-dimethylimidazol-2-ylidene) in place of IPr were examined using density functional theory (DFT), with the BVP86 functional, the LANL2TZ(f) basis set for metal centers, and the 6-311G+(d) basis set for nonmetal atoms. As demonstrated previously with (IMe)Cu–Fp, (IMe)Cu–Mp, and related complexes, this level of theory provided excellent correlation with experimentally determined structural parameters and vibrational frequencies. Calculated bond distances are presented in Table 2 for comparison to the IPr derivatives, and

Table 2. Calculated Bond Distances for (IMe)Cu–[M] Model Complexes[a]

complex[b]	d(Cu–M) (Å)/FSR[c]	d(Cu···CO) (Å)[d]
(IMe)Cu–Fp[e]	2.330/0.997	*2.490*, *2.574*
(IMe)Cu–Rp	2.441/1.011	*2.739*, *2.755*
(IMe)Cu–Wp	2.535/1.025	*1.971*, *1.971*, *1.975*
(IMe)Cu–Mc	2.408/1.028	*2.434*, *2.434*, 3.054, 3.055
(IMe)Cu–Mp[e]	2.588/1.050	*2.194*, *2.196*, 3.640
(IMe)Cu–Crp	2.468/1.052	*2.172*, *2.172*, 3.556
(IMe)Cu–Cc	2.315/0.994	*2.486*, *2.501*, *2.660*, 4.086

[a]BVP86/LANL2TZ(f)/6-311+G(d). [b]Decreasing order of $[M]^-$ nucleophilicity; see ref 11. [c]Formal shortness ratio; see ref 22. [d]Only distances within van der Waals contact (<4.2 Å)[24] are listed. Italicized values represent semibridging carbonyls ($0.1 < \alpha < 0.6$), and nonitalicized values represent terminal carbonyls ($\alpha \geq 0.6$); see ref 25. [e]Data taken from ref 4.

calculated vibrational data for the CO ligands is presented in Supporting Information. The optimized structures for the IMe-supported heterobimetallic complexes featuring Fe, Ru, Mo, and Cr closely matched experimental observations for the IPr-supported complexes in terms of Cu–M distances, semibridging CO distances, and number of semibridging CO interactions (see Tables 1 and 2). The trends in Cu–M FSR values, including the anomalous value for the Cu–Co bond, were successfully replicated by the DFT analysis. The optimized structure for (IMe)Cu–Wp closely matched the (IPr)Cu–Wp structure with the linear Cu–W–Cp(centroid) angle, shorter Cu–W distance, and three semibridging CO ligands rather than two (Figure 3b). The outliers were the Mn (Figure 3b) and Co cases: (IMe)Cu–Cc and (IMe)Cu–Mc were calculated to have three and two semibridging CO ligands, respectively, whereas, experimentally, this trend was reversed for the IPr series. This distinction apparently had little effect on the calculated Cu–Mn and Cu–Co distances, which agreed quite well with the experimental values. The latter observation implies that the semibridging CO interactions do not influence the Cu–M distances to a large extent.

The frontier molecular orbitals for the expanded heterobimetallic series closely mimic the previously published frontier orbitals for (IMe)Cu–Fp.[4] As an example, selected orbital surfaces for (IMe)Cu–Mc are plotted on a computationally determined energy scale in Figure 4. A general pattern is largely conserved throughout the series. For each complex, the three

dx.doi.org/10.1021/ic5019778 | *Inorg. Chem.* 2014, 53, 11307–11315

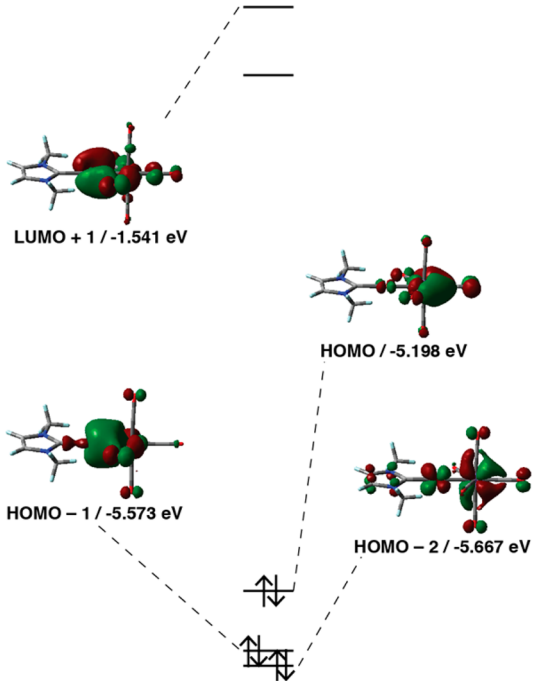

Figure 4. Frontier molecular orbital diagram calculated for (IMe)Cu–Mc (BVP86/LANL2TZ(F)/6-311+G(d), 0.04 isocontours). In this case, the HOMO and HOMO-2 orbitals possess Cu–Mn π*-character, the HOMO-1 orbital possesses Cu–Mn σ-character, the LUMO (not shown) does not involve Cu–Mn or Cu–CO interactions, and the LUMO+1 exhibits Cu–CO through-space overlap.

highest-lying filled molecular orbitals (MOs) have closely spaced energies; one possesses Cu–M σ-character and the other two possess Cu–M π*-character. The effect of the filled Cu–Fe π* MOs in (IPr)Cu–Fp has been detected spectroscopically.[4b] A low-lying empty MO exhibits significant through-space overlap between Cu and the semibridging CO ligands, and the relevant MO of Cu–M σ*-character is invariably quite high in energy (LUMO+3 or higher).

Charge distribution in the heterobimetallic series was probed using natural population analysis (Table 3). Contrary to our expectations, both the calculated Cu atomic charges and the calculated [(IMe)Cu] fragment charges were relatively invariant across the series, despite the extreme differences in relative nucleophilicities and reduction potentials of the [$MCp_n(CO)_m$] partners. The calculated charge of Cu ranged only from 0.37 to 0.45 e across the series, and the calculated fragment charge of [(IMe)Cu] ranged only from 0.61 e to 0.72 e. Furthermore, no discernible trends were evident.

Table 3. Calculated Charges (q) from Natural Population Analysis for (IMe)Cu–$MCp_n(CO)_m$ Model Complexes[a]

complex[b]	q[Cu]	q[M]	q[(IMe)Cu]	q[$MCp_n(CO)_m$]
(IMe)Cu–Fp[c]	0.39	−1.19	0.63	−0.63
(IMe)Cu–Rp	0.40	−1.05	0.61	−0.61
(IMe)Cu–Wp	0.40	−0.95	0.69	−0.69
(IMe)Cu–Mc	0.45	−2.22	0.68	−0.68
(IMe)Cu–Mp[c]	0.45	−1.19	0.72	−0.72
(IMe)Cu–Crp	0.43	−1.66	0.70	−0.70
(IMe)Cu–Cc	0.37	−1.41	0.65	−0.65

[a]BVP86/LANL2TZ(f)/6-311+G(d). [b]Decreasing order of $[M]^-$ nucleophilicity; see ref 11. [c]Data taken from ref 4.

While the fragment charge of [$MCp_n(CO)_m$] was necessarily invariant as well, the calculated charge of M did span a large range, from −0.95 to −2.22 e. Within both the group 6 series and the group 8 series, the atomic charge of M became less anionic going down the triad, tracking with the trends in metal electronegativities. No discernible trend was evident across the 3*d* series, with regard to the electronegativity of M. Instead, the dominant trend was with number of CO ligands, with a greater number of CO ligands generally stabilizing more anionic charge localized on M. The negative charge localization on the metal centers was counterbalanced by positive charge delocalization in the Cp rings and, especially, by positive charge localization on CO carbon atoms (see the Supporting Information). Once again, the (IMe)Cu–Cc complex was an outlier, as the Co center was calculated to hold less anionic charge than expected based on the number of CO ligands. This anomaly could be tied to the unusually short Cu–Co bond distance resulting in negative charge transfer from Co toward Cu.

NBO analysis of the Fe, W, Mn, Mo, and Cr derivatives underscored the ionic nature of the Cu–M bonds. In all of these cases, significant (3–4%) non-Lewis occupancies were calculated, and no Cu–M bonding NBOs were located in any of these cases. Instead, significant M → Cu donor–acceptor interactions were identified, with the two predominant acceptor orbitals being Cu valence (∼85% Cu 4p) and Cu–C_{NHC} antibonding (∼65–70% Cu 4s) in nature. For the Ru and Co cases, Cu–M bonding NBOs were located. For the Ru derivative, this bonding NBO was 13% Cu $sp^{0.07}d^{0.09}$ and 87% Ru $sp^{0.79}d^{6.17}$ in nature; for the Co derivative, this bonding NBO was 20% Cu $sp^{0.72}d^{0.09}$ and 80% Co $sp^{2.66}d^{1.75}$ in nature. Apparently, the Cu–Ru and Cu–Co bonds are unusually covalent, according to NBO analysis, compared to the other Cu–M bonds. In the Co case, there may be a link between this finding and the anomalously small Cu–Co FSR and anomalously positive Co partial charge values.

Wiberg bond index (WBI) values were calculated to further probe covalency of the bonding in the heterobimetallic series (Table 4). The (IMe)Cu–[M] complexes constructed with the strongest nucleophiles, $[Fp]^-$ and $[Rp]^-$, were calculated to have higher Cu–M bond indices. These values were significantly ≪1, indicating that the Cu–Fe and Cu–Ru bonds possess low covalent character and are best-viewed as polar bonds with significant ionic character. The WBI values decreased even further for the weaker nucleophiles, but the

Table 4. Wiberg Bond Indices for (IMe)Cu–$MCp_n(CO)_m$ Model Complexes[a]

complex[b]	Cu–M	Cu–C_{NHC}	Cu···CO	M–CO
(IMe)Cu–Fp[c]	0.39	0.58	0.15, 0.13	1.20, 1.18
(IMe)Cu–Rp	0.40	0.57	0.11, 0.11	1.27, 1.27
(IMe)Cu–Wp	0.29	0.63	0.21, 0.21, 0.17	1.38, 1.38, 1.36
(IMe)Cu–Mc	0.28	0.58	0.17, 0.17, 0.05, 0.05, 0.03	1.08, 1.08, 1.06, 1.04, 1.04
(IMe)Cu–Mp[c]	0.28	0.59	0.24, 0.24, 0.02	1.33, 1.33, 1.29
(IMe)Cu–Crp	0.30	0.58	0.25, 0.25, 0.02	1.20, 1.20, 1.18
(IMe)Cu–Cc	0.32	0.60	0.18, 0.18, 0.13, 0.03	2.13, 2.10, 2.07, 2.06

[a]BVP86/LANL2TZ(f)/6-311+G(d). [b]Decreasing order of $[M]^-$ nucleophilicity; see ref 11. [c]Data taken from ref 4.

dx.doi.org/10.1021/ic5019778 | Inorg. Chem. 2014, 53, 11307–11315

difference was minor and all the Cu−M WBI values span a very small range across the series. Small but significant WBI values were calculated for the semibridging Cu···CO interactions and corroborated their independent assignment using the structural asymmetry parameter, α (*vide supra*). The number of semibridging CO ligands identified using the α parameter matched the number of close Cu···CO contacts having non-negligible WBI values in all cases.

Structural Isomerism of IMes Complexes. Our previous conditions for synthesizing (IMes)Cu−Fp (1:1 (IMes)CuCl: $[Fp]^-$ at room temperature) were sufficient to produce (IMes)Cu−Rp and (IMes)Cu−Wp in yields of 64% and 88%, respectively. None of these three complexes has yet provided X-ray-quality crystals, despite repeated attempts using a variety of different crystallization solvents and conditions. With the weaker nucleophiles, more forcing conditions were necessary to achieve complete consumption of the (IMes)CuCl starting material. As described below, the available evidence indicates that these (IMes)Cu−[M] complexes exist in solution equilibrium with their $\{(IMes)_2Cu\}\{Cu[M]_2\}$ isomers for [M] = Mc, Mp, Crp, and Cc (Figure 5a).

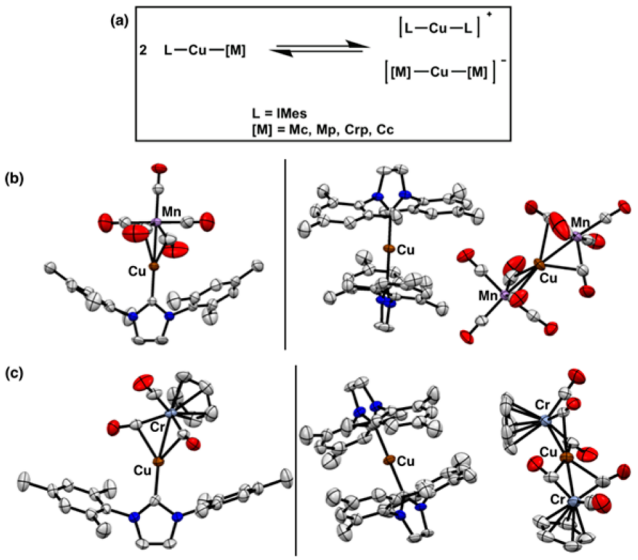

Figure 5. (a) Solution equilibrium between neutral, (IMes)Cu-[M], and ionic, $\{(IMes)_2Cu\}\{Cu[M]_2\}$, isomers. Corresponding solid-state structures of (b) Mc and (c) Crp derivatives as 50% probability thermal ellipsoids. Hydrogen atoms and co-crystallized solvent molecules have been omitted.

In the case of the Mn derivative, incomplete consumption of (IMes)CuCl was observed by reacting a 1:1 mixture of (IMes)CuCl and Na^+Mc^- at room temperature. Complete consumption of (IMes)CuCl was achieved either by reacting a 1:3 mixture of these reactants at room temperature or by reacting a 1:1.2 mixture at 36 °C. Analysis of the crystals from these two reaction conditions by single-crystal XRD yielded different results (Figure 5b). The crystals grown from the mixture with excess Na^+Mc^- were identified as (IMes)Cu−Mc by X-ray crystallography, while the crystals grown from the mixture with equimolar Na^+Mc^- were identified as $\{(IMes)_2Cu\}\{Cu(Mc)_2\}$ by X-ray crystallography. Interestingly, the crystallization conditions and solvent systems were identical in both cases. While the solid-state IR spectra of these samples were different, dissolution of both types of crystals in C_6D_6 gave identical ^1H and $^{13}C\{^1H\}$ NMR spectra (presumably time-averaged). Furthermore, the ^1H NMR chemical shifts and line widths were temperature-dependent (see the Supporting Information). As a result, we propose that the two isomers, (IMes)Cu−Mc and $\{(IMes)_2Cu\}\{Cu(Mc)_2\}$, exist in solution equilibrium, and that one form or the other can be crystallized selectively with the presence or absence of excess Na^+Mc^-. IR analysis in toluene solution of both (IMes)Cu−Mc and $\{(IMes)_2Cu\}\{Cu(Mc)_2\}$ gave identical spectra (see Figure S2 in the Supporting Information) closely matching the solid-state IR spectrum of (IMes)Cu−Mc. This observation is consistent with the neutral (IMes)Cu−Mc isomer dominating in toluene solution, although it is likely that the position of the equilibrium will be highly solvent-dependent. Analogous behavior was observed for the Crp (Figure 5c) and Mp (see Figures S3 and S4 in the Supporting Information) derivatives. Related to this behavior, it has been reported previously that neutral (IMes)AgCl complexes are in solution equilibrium with ionic $\{(IMes)_2Ag\}\{AgCl_2\}$ isomers, while neutral (IPr)AgCl isomerizes to a negligible extent under standard conditions.[27]

In the case of the weakest nucleophile, $[Cc]^-$, the ion pair $\{(IMes)_2Cu\}\{Cu(Cc)_2\}$ was crystallized, regardless of the different stoichiometric ratios and temperatures of synthesis that we canvassed (Figure 6). Similarly, a previous report of an

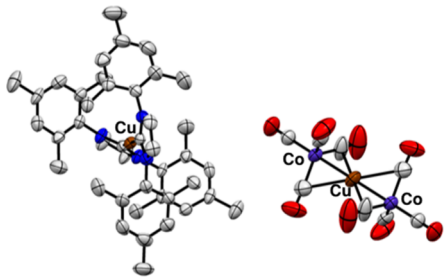

Figure 6. Solid-state structure of $\{(IMes)_2Cu\}\{Cu(Cc)_2\}$ as 50% probability thermal ellipsoids. Hydrogen atoms and co-crystallized solvent molecules have been omitted.

attempted synthesis of (dmpe)Cu−Cc resulted, instead in $\{(dmpe)_2Cu\}\{Cu(Cc)_2\}$.[28] This observation can be combined with the fact that (dmpe)Cu−Fp is unstable at room temperature[29] to highlight the importance of bulky carbene ligands compared to either smaller carbenes or bulky phosphines. Bulky phosphines such as dmpe are less capable of stabilizing heterobimetallic Cu−[M] bonding, and small carbenes such as IMes give heterobimetallic Cu−[M] complexes that are prone to isomerization through ligand redistribution, particularly when $[M]^-$ is a weak nucleophile. On the other hand, bulky carbenes such as IPr support a wide range of heterobimetallic Cu−[M] complexes that are robust toward thermal decomposition, as well as structural isomerism.

CONCLUSIONS

In conclusion, a new series of Cu−M heterobimetallic complexes supported by *N*-heterocyclic carbene ligands has been synthesized, characterized crystallographically, and analyzed computationally. The bulky IPr carbene is particularly well-suited to stabilize a wide range of Cu−M bonding as well as prevent isomerization through ligand redistribution. Future stoichiometric and catalytic reactivity studies stand to leverage the tunable kinetic and thermodynamic parameters available

dx.doi.org/10.1021/ic5019778 | *Inorg. Chem.* 2014, 53, 11307−11315

upon construction of the heterobimetallic toolbox presented here with precise control over structure−function relationships.

EXPERIMENTAL SECTION

General Considerations. All reactions and manipulations were conducted under purified N_2 using standard Schlenk line techniques or in a glovebox. Reaction solvents (THF, toluene, diethyl ether, dichloromethane, acetonitrile, pentane) were purified using a Glass Contour Solvent System built by Pure Process Technology, LLC. Deuterated solvents (C_6D_6, CD_3CN, CD_2Cl_2, toluene-d_8) were degassed by repeated freeze−pump−thaw cycles and stored over activated 3-Å molecular sieves prior to use. ^1H and ^{13}C NMR spectra were recorded using Bruker Avance 400-MHz or 500-MHz NMR spectrometers. NMR spectra were recorded at room temperature unless otherwise indicated, and chemical shifts were referenced to residual solvent peaks. FT-IR spectra were recorded in a glovebox on powder samples using a Bruker ALPHA spectrometer fitted with a diamond-ATR detection unit. Elemental analyses were performed by Midwest Microlab, LLC, in Indianapolis, IN. Single-crystal X-ray diffraction (XRD) studies were performed using a Bruker SMART X2S benchtop diffractometer fitted with a Oxford Cryostreams Desktop Cooler. Solution and refinement was accomplished with the SHELXTL suite of programs,[30] using standard methods,[31] and CIF files are included as Supporting Information. Literature methods were used to synthesize NaWp,[32] IMes·HCl, IPr·HCl,[33] (IMes)CuCl, (IPr)CuCl,[34] (IMes)CuFp, (IPr)CuFp, and (IPr)CuMp.[4]

Computational Methods. All calculations were performed using Gaussian 09, Revision B.01.[35] Density functional theory (DFT) calculations were carried out using a hybrid functional, BVP86, consisting of Becke's 1988 gradient-corrected Slater exchange functional[36] combined with the VWN5 local electron correlation functional and Perdew's 1986 nonlocal electron correlation functional.[37] Mixed basis sets were employed: the LANL2TZ(f) triple-ζ basis set[38] with effective core potential[39] was used for all transition metals, and the Gaussian 09 internal 6-311+G(d) basis set was used for all other atom types. Structural geometries were optimized to energy minima, and then frequency calculations were performed to confirm that no imaginary frequencies were present. Natural population analysis was used to determine atomic and fragment charges, and Wiberg bond indices were used to determine bond orders. Both were obtained from NBO v. 3.1[40] calculations within Gaussian 09. Optimized structures of (IMe)Cu−Fp and (IMe)Cu−Mp were reported previously;[4] other optimized coordinates are provided as Supporting Information.

Preparation of NaRp. Sodium (0.0425 g, 1.85 mmol) was mixed with mercury to generate a 5% Na/Hg amalgam in a scintillation vial. Separately, $[CpRu(CO)_2]_2$ (0.328 g, 0.739 mmol) was dissolved in THF (15 mL) in another scintillation vial and then transferred into the vial with the amalgam. The solution was stirred vigorously at room temperature overnight, during which time the solution color changed from orange to brown. The solution was then pipet-filtered through Celite and dried *in vacuo* to give a small quantity of orange solid that was used without further purification. ^1H NMR (400 MHz, CD_3CN): δ 4.87. During the course of this study, a reliable and high-yielding preparation of KRp with thorough characterization data was published.[21]

Preparation of NaMp. $Mo(CO)_6$ (2.0 g, 7.57 mmol) and a magnetic stirrer were placed into 250-mL three-neck flask fitted with a reflux condenser and connected to a Schlenk line. The system was purged several times by vacuum/N_2 cycles, followed by the addition of dry/degassed 1,2-dimethoxyethane (50 mL). NaC_5H_5 (2.0 M in THF, 3.75 mL, 7.57 mmol) then was added by cannula and the mixture was refluxed at 80 °C overnight. The solvent was removed *in vacuo* to leave a light yellow powder. Yield: 1.8 g, 6.7 mmol, 88%. ^1H NMR (400 MHz, CD_3CN): δ 5.0. ^{13}C NMR (400 MHz, CD_3CN): δ 86.1. IR (solid, cm^{-1}): 1888 (ν_{CO}), 1762 (ν_{CO}), 1663 (ν_{CO}).

Preparation of NaCrp. An existing literature preparation was adapted.[41] A modified 500-mL, 3-neck round-bottom flask with one female joint was fitted with a reflux condenser, a rubber septum, and a small round-bottom flask. The system was evacuated and purged with N_2. A solution of NaCp (2.0 M in THF, 19 mL, 38 mmol) was added by syringe, and the solution was evaporated to dryness *in vacuo*. Under a flow of N_2, $Cr(CO)_6$ (8.34 g, 37.9 mmol) was added, followed by di-*n*-butyl ether (100 mL). The solution was heated to a reflux for 12 h. After cooling the solution to room temperature, a yellow precipitate remained. The small round-bottom flask was replaced with a 100-mL Schlenk frit, and the solution was filtered. The yellow solid that was collected was then washed with di-*n*-butyl ether (3 × 10 mL) and hexanes (3 × 10 mL). The yellow solid was sublimed at 60 °C to remove residual $Cr(CO)_6$, and then used without further purification. Yield: 7.88 g, 35.2 mmol, 93%. ^1H NMR (500 MHz, CD_3CN): δ 4.42 (s, Cp). IR (solid, cm^{-1}): 1861 (ν_{CO}), 1687 (ν_{CO}), 1002, 809, 695, 664, 513.

Preparation of NaCc. Sodium (0.700 g, 30.4 mmol) was mixed with mercury to generate a 5% Na/Hg amalgam in a 250-mL round-bottom flask. Tetrahydrofuran (THF) (50 mL) was added to the amalgam, followed by $Co_2(CO)_8$ (2.0 g, 5.8 mmol). The solution was stirred vigorously at room temperature for 2 h, during which the solution color changed from red to brown. The solution was then decanted onto a pad of Celite and filtered. The Celite pad was washed with additional THF (25 mL). The combined filtrates were evaporated to dryness *in vacuo* for 12 h, providing a brown solid. Yield: 2.36 g, 12.2 mmol, 104%. Note: the >100% yield is likely due to the presence of THF molecules coordinated to Na, which was not quantified. This material was used for subsequent procedures without further purification. IR (solid, cm^{-1}): 2981, 2877, 1915 (ν_{CO}), 1848 (br ν_{CO}), 1459, 1047, 895, 548.

Preparation of NaMc. An analogous procedure to the preparation of NaCc was used, but with $Mn_2(CO)_{10}$ (2.0 g, 5.1 mmol) in place of $Co_2(CO)_8$. Yield: 2.35 g, 10.8 mmol, 105%. Note: the >100% yield is likely due to the presence of THF molecules coordinated to Na, which was not quantified. This material was used for subsequent procedures without further purification. IR (solid, cm^{-1}): 2979, 2878, 1932 (ν_{CO}), 1881 (ν_{CO}), 1813 (br ν_{CO}), 1042, 662, 655.

Preparation of (IPr)CuRp. A solution of NaRp (0.0452 g, 0.184 mmol) in THF (5 mL) was added to a suspension of (IPr)CuCl (0.0899 g, 0.184 mmol) in THF (5 mL) in a scintillation vial. The mixture was stirred at room temperature overnight, during which time a color change from orange to brown, concomitant with formation of a brown precipitate, was observed. The mixture was then pipet-filtered through Celite and dried *in vacuo* to give an orange solid. Analytically pure crystals were obtained by diffusion of pentane vapors into a concentrated and filtered toluene solution at −36 °C. Yield: 0.0904 g, 0.134 mmol, 73%. ^1H NMR (500 MHz, C_6D_6): δ 7.24 (t, J = 7.5 Hz, 2H, *p*-H), 7.12 (d, J = 7.5 Hz, 4H, *m*-H), 6.27 (s, 2H, NCH), 4.68 (s, Cp), 2.66 (sept., J = 7.0 Hz, 4H, C$\underline{H}$(CH$_3$)$_2$), 1.50 (d, J = 7.0 Hz, 12H, CH(C$\underline{H}_3$)$_2$), 1.11 (d, J = 7.0 Hz, 12H, CH(C$\underline{H}_3$)$_2$). $^{13}C\{^1H\}$ NMR (500 MHz, C_6D_6): δ 207.7 (CO), 182.5 (NCCu), 146.0, 135.2, 130.7, 124.3, 121.7, 81.3 (Cp), 29.1, 24.7, 24.0. IR (solid, cm^{-1}): 2962, 1940 (ν_{CO}), 1867 (ν_{CO}), 1470, 1455, 803, 791, 757, 739. Anal. Calcd for $C_{34}H_{41}CuN_2O_2Ru$: C, 60.56; H, 6.13; N, 4.15. Found: C, 60.81; H, 6.02; N, 4.34.

Preparation of (IPr)CuWp. A 250-mL round-bottom flask equipped with a stir bar was charged with (IPr)CuCl (0.745 g, 1.53 mmol) and THF (20 mL). To this slurry, a solution of NaWp (0.544 g, 1.53 mmol) in THF (15 mL) was added. The red-orange solution was stirred overnight at room temperature. The resulting cloudy yellow-brown solution was filtered through a bed of Celite and then evaporated to dryness at reduced pressure. The remaining oily brown solid was dissolved in diethyl ether (15 mL) and evaporated to dryness to obtain the product as a yellow solid. Yield: 1.102 g 1.40 mmol, 91%. ^1H NMR (400 MHz, C_6D_6): δ 7.25 (t, J = 8.0 Hz, 2H, *p*-CH), 7.14 (d, *m*-CH, partial overlap with solvent peak), 6.38 (s, 2H, NCH), 4.68 (s, 5H, Cp), 2.80 (sept., J = 7.0 Hz, 4H, C$\underline{H}$(CH$_3$)$_2$), 1.51 (d, J = 7.0 Hz, 12H, CH(C$\underline{H}_3$)$_2$), 1.08 (d, J = 7.0 Hz, 12 H, CH(C$\underline{H}_3$)$_2$). $^{13}C\{^1H\}$ NMR (500 MHz, C_6D_6): δ 219.3 (CO), 186.4 (NCCu), 145.9, 135.4, 130.7, 124.4, 122.9, 85.6 (Cp), 29.0, 24.7, 24.1. IR (solid, cm^{-1}): 2963, 1920 (ν_{CO}), 1818 (ν_{CO}), 1784 (ν_{CO}), 1457, 1328, 799, 743, 582. Anal.

dx.doi.org/10.1021/ic5019778 | *Inorg. Chem.* 2014, 53, 11307−11315

Calcd for $C_{35}H_{41}CuN_2O_3W$: C, 53.54; H, 5.26; N, 3.57. Found: C, 53.88; H, 5.33; N, 3.46.

Preparation of (IPr)CuMc. A solution of (IPr)CuCl (0.200 g, 0.410 mmol) in THF (50 mL) was added to a solution of NaMc (0.2679 g, 1.23 mmol) in THF (20 mL), and the resulting mixture was stirred at room temperature for 24 h. The mixture was then filtered through a pad of Celite and evaporated to dryness, giving a dark brown-green solid. Analytically pure crystals were obtained by diffusion of pentane vapors into a concentrated and filtered toluene solution at −36 °C. Yield: 0.225 g, 0.347 mmol, 85%. ^{1}H NMR (500 MHz, C_6D_6): δ 7.24 (t, J = 10 Hz, 2H, p-CH), 7.09 (d, J = 5 Hz, 4H, m-CH), 6.24 (s, 2H, NCH), 2.57 (sept., J = 6.3 Hz, 4H, C$\underline{H}$(CH$_3$)$_2$), 1.41 (d, J = 5 Hz, 12H, CH(C$\underline{H}_3$)$_2$), 1.06 (d, J = 10 Hz, 12H, CH(C$\underline{H}_3$)$_2$). ^{13}C{^{1}H} NMR (500 MHz, C_6D_6): δ 223.8 (CO), δ 181.2 (NCCu), 145.6, 134.8, 130.9, 124.5, 122.8, 29.0, 24.6, 24.0. IR (solid, cm^{-1}): 2968, 2042 (ν_{CO}), 1885 (ν_{CO}), 1830 (ν_{CO}), 1459, 1043, 806, 760, 740, 686, 662, 650. Anal. Calcd for $C_{32}H_{36}CuMnN_2O_5$: C, 59.39; H, 5.61; N, 4.33. Found: C, 58.92; H, 5.59; N, 4.50.

Preparation of (IPr)CuCrp. A solution of (IPr)CuCl (0.100 g, 0.204 mmol) in THF (50 mL) was added to a solution of NaCrp (0.1644 g, 0.612 mmol) in THF (10 mL), and the resulting mixture was stirred at 36 °C overnight. The resulting mixture was filtered through a pad of Celite and evaporated to dryness, giving a yellow solid. Crystals were obtained by diffusion of pentane vapors into a concentrated and filtered toluene solution at −36 °C. Yield: 0.110 g, 0.159 mmol, 78%. ^{1}H NMR (500 MHz, C_6D_6): δ 7.19 (t, J = 7.5 Hz, 2H, p-CH), 7.09 (d, J = 2.5 Hz, 4H, m-CH), 6.35 (s, 2H, NCH), 4.20 (s, Cp), 2.75 (sept., J = 7.5 Hz, 4H, C$\underline{H}$(CH$_3$)$_2$), 1.42 (d, J = 5 Hz, 12H, CH(C$\underline{H}_3$)$_2$), 1.05 (d, J = 5 Hz, 12H, CH(CH$_3$)$_2$). ^{13}C{^{1}H} NMR (500 MHz, C_6D_6): δ 160.0 (NCCu), 145.7, 135.1, 130.5, 124.2, 122.4, 82.8 (Cp), 28.7, 24.4, 23.8. Note: no peak corresponding to bound CO was located. IR (solid, cm^{-1}): 2963, 1914 (ν_{CO}), 1822 (ν_{CO}), 1792 (ν_{CO}), 1459, 803, 757, 635. Anal. Calcd for $C_{35}H_{41}CrCuN_2O_3$: C, 64.35; H, 6.33; N, 4.29. Found: C, 64.48; H, 6.34; N, 4.26.

Preparation of (IPr)CuCc. A solution of (IPr)CuCl (0.100 g, 0.204 mmol) in THF (30 mL) was added to a solution of NaCc (0.0476 g, 0.246 mmol) in THF (10 mL), and the resulting mixture was stirred at 36 °C overnight. The mixture was then filtered through a pad of Celite and evaporated to dryness, giving a dark brown solid. Analytically pure crystals were obtained by diffusion of pentane vapors into a concentrated and filtered solution in toluene at −36 °C. Yield: 0.106 g, 0.170 mmol, 83%. ^{1}H NMR (500 MHz, C_6D_6): δ 7.23 (t, J = 7.5 Hz, 2H, p-CH), 7.08 (d, J = 5 Hz, 4H, m-CH), 6.29 (s, 2H, NCH), 2.59 (sept., J = 6.3 Hz, 4H, C$\underline{H}$(CH$_3$)$_2$), 1.38 (d, J = 5 Hz, 12H, CH(C$\underline{H}_3$)$_2$), 1.05 (d, J = 2.5 Hz, 12H, CH(C$\underline{H}_3$)$_2$). ^{13}C{^{1}H} NMR (500 MHz, C_6D_6): δ 160.3 (NCCu), 145.4, 134.9, 131.0, 124.5, 122.7, 29.0, 24.5, 24.2. Note: no peak corresponding to bound CO was located. IR (solid, cm^{-1}): 2966, 2928, 2870, 2038 (ν_{CO}), 1957 (ν_{CO}), 1915 (ν_{CO}), 1458, 806, 761, 737, 554, 538. Anal. Calcd for $C_{31}H_{36}CoCuN_2O_4$: C, 59.75; H, 5.82; N, 4.50. Found: C, 60.01; H, 5.73; N, 4.43.

Preparation of (IMes)CuRp. A solution of NaRp (0.150 g, 0.612 mmol) in THF (10 mL) was added to a suspension of (IMes)CuCl (0.246 g, 0.612 mmol) in THF (10 mL) in a round-bottom flask. The mixture was stirred at room temperature overnight, during which time a color change from orange to brown, concomitant with formation of a brown precipitate, was observed. The mixture was then pipet-filtered through Celite and dried *in vacuo* to give an orange solid. Analytically pure material was obtained by diffusion of pentane vapors into a concentrated and filtered toluene solution at −36 °C. Yield: 0.2302 g, 0.390 mmol, 64%. ^{1}H NMR (500 MHz, C_6D_6): 6.78 (s, 4H, m-H), 6.00 (s, 2H, NCH), 4.75 (s, Cp), 2.09 (s, 6H, p-CH$_3$), 2.06 (s, 12H, o-CH$_3$). ^{13}C{^{1}H} NMR (500 MHz, C_6D_6): 207.9 (CO), 181.1 (NCCu), 139.3, 135.8, 135.0, 129.5, 120.7, 81.2 (Cp), 21.0, 17.8. IR (solid, cm^{-1}): 1932 (ν_{CO}), 1863 (ν_{CO}), 1486, 788. Anal. Calcd for $C_{28}H_{29}CuN_2O_2Ru$: C, 56.99; H, 4.95; N, 4.75. Found: C, 52.99; H, 4.74; N, 4.25. Although satisfactory combustion analysis data were not obtained after multiple attempts, NMR and IR data are included in the Supporting Information as indications of purity.

Preparation of (IMes)CuWp. A 250-mL round-bottom flask equipped with a stir bar was charged with (IMes)CuCl (0.760 g, 1.88 mmol) and THF (20 mL). To this slurry a solution of NaWp (0.670 g, 1.88 mmol) in THF (20 mL) was added. The red-orange solution was stirred overnight at room temperature. The resulting cloudy yellow-brown solution was filtered through a bed of Celite and evaporated to dryness under reduced pressure. The remaining yellow-orange oily residue was dissolved in diethyl ether (15 mL) and evaporated to yield a fine yellow-orange solid. Yield: 1.162 g 1.65 mmol, 88%. ^{1}H NMR (400 MHz, C_6D_6): δ 6.81 (s, 4H, m-CH), 6.04 (s, 2H, NCH), 4.68 (s, 5H, Cp), 2.13, 2.10 (two overlapping singlets, 18H, o,p-CH$_3$), ^{13}C{^{1}H} NMR (400 MHz, C_6D_6): δ 219.4 (CO), 139.4, 135.7, 135.2, 129.6, 121.5, 85.6 (Cp), 21.1, 17.7. IR (solid, cm^{-1}): 1900 (ν_{CO}), 1770 (ν_{CO}), 1485, 1238, 852, 799, 571. Although combustion analysis data were not obtained after multiple attempts, NMR and IR data are included in the Supporting Information as indications of purity.

Crystallization of (IMes)CuMc. A solution of (IMes)CuCl (0.100 g, 0.248 mmol) in THF (40 mL) was added to a solution of NaMc (0.162 g, 0.744 mmol) in THF (40 mL), and the resulting mixture was stirred overnight at room temperature. The mixture was then filtered through a pad of Celite and evaporated to dryness, giving a brown-green solid. Analytically pure crystals were obtained by diffusion of pentane vapors into a concentrated and filtered toluene solution at −36 °C. Yield: 0.0875 g, 0.155 mmol, 63%. IR (solid, cm^{-1}): 2045 (ν_{CO}), 1940 (ν_{CO}), 1875 (ν_{CO}), 1485, 1029, 852, 799, 739, 650. Anal. Calcd for $C_{26}H_{24}CuMnN_2O_5$: C, 55.47; H, 4.30; N, 4.98. Found: C, 55.27; H, 4.45; N, 4.99.

Crystallization of {(IMes)$_2$Cu}{Cu(Mc)$_2$}. A solution of (IMes)CuCl (0.100 g, 0.247 mmol) in THF (30 mL) was added to a solution of NaMc (0.0644 g, 0.296 mmol) in THF (10 mL), and the resulting mixture was stirred overnight at 36 °C. The mixture was then filtered through a pad of Celite and evaporated to dryness, giving a light green-brown solid. Analytically pure crystals were obtained by diffusion of pentane vapors into a concentrated and filtered toluene solution at −36 °C. Yield: 0.1232 g, 0.109 mmol, 44%. IR (solid, cm^{-1}): 2031 (ν_{CO}), 1937 (ν_{CO}), 1885 (ν_{CO}), 1484, 1236, 836, 740, 651. Anal. Calcd for $C_{52}H_{48}Cu_2Mn_2N_4O_{10}$: C, 55.47; H, 4.30; N, 4.98. Found: C, 56.09; H, 4.40; N, 5.00.

Solution Characterization Data for the Mc Derivatives Supported by IMes. ^{1}H NMR (room temperature, 500 MHz, C_6D_6): δ 6.76 (s, 4H, m-CH), 5.92 (s, 2H, NCH), 2.08 (s, 6H, p-CH$_3$), 1.97 (s, 12H, o-CH$_3$). ^{13}C{^{1}H} NMR (500 MHz, C_6D_6): δ 224.2 (CO), δ 179.3 (NCCu), 139.6, 135.3, 134.7, 129.6, 121.2, 25.8, 21.0, 17.5, 17.0. IR (toluene solution, cm^{-1}): 2046 (ν_{CO}), 1951 (ν_{CO}), 1909 (ν_{CO}).

Preparation of (IMes)CuMp. In the glovebox, a 20-mL scintillation vial was charged with NaMp (0.1 g, 0.373 mmol) and (IMes)CuCl (0.0752 g, 0.186 mmol). The solids were then dissolved in THF (10 mL). The reaction mixture was stirred at room temperature for 36 h. The resulting light yellow solution was filtered through a plug of Celite, and the solvent was removed *in vacuo*. Yield: 0.092 g, 0.148 mmol, 79%. IR (solid, cm^{-1}): 1920 (ν_{CO}), 1823 (ν_{CO}), 1792 (ν_{CO}). Although combustion analysis data were not obtained after multiple attempts, NMR and IR data are included in the Supporting Information as indications of purity.

Preparation of {(IMes)$_2$Cu}{Cu(Mp)$_2$}. In the glovebox, a 20-mL scintillation vial was charged with NaMp (0.1 g, 0.373 mmol) and (IMes)CuCl (0.15 g, 0.373 mmol). The solids were then dissolved in THF (10 mL). The reaction mixture was stirred at room temperature for 24 h. The reaction mixture was filtered through a plug of Celite, and the solvent was removed in vacuo. Yield: 0.110 g, 132 mmol, 24%. IR (solid, cm^{-1}): 1931 (ν_{CO}), 1912 (ν_{CO}), 1817 (ν_{CO}), 1775 (ν_{CO}). Although combustion analysis data were not obtained after multiple attempts, NMR and IR data are included in the Supporting Information as indications of purity.

Solution Characterization Data for the Mp Derivatives Supported by IMes. ^{1}H NMR (400 MHz, C_6D_6): δ 6.79 (s, 4H, m-CH), 6.01 (s, 2H, NCH), 4.77 (s, Cp), 2.10 (s, 12H, o-CH$_3$), 2.08 (s, 6H, p-CH$_3$). ^{13}C{^{1}H} NMR (400 MHz, C_6D_6): δ 229.8 (CO), 139.5, 135.7, 129.7, 121.4, 87.5 (Cp), 21.2, 17.7.

Crystallization of (IMes)CuCrp. A solution of (IMes)CuCl (0.100 g, 0.248 mmol) in THF (40 mL) was added to a solution of NaCrp (0.1368 g, 0.610 mmol) in THF (20 mL), and the resulting mixture was stirred overnight at room temperature. The mixture was then filtered through a pad of Celite and evaporated to dryness, giving a yellow solid. Crystals were obtained by diffusion of pentane vapors into a concentrated and filtered toluene solution at −36 °C. Yield: 0.089 g, 0.156 mmol, 63%. IR (solid, cm^{-1}): 1914 (ν_{CO}), 1821 (ν_{CO}), 1784 (ν_{CO}), 851, 806, 738, 636. Anal. Calcd for $C_{29}H_{29}CrCuN_2O_3$: C, 61.20; H, 5.14; N, 4.92. Found: C, 61.46; H, 5.18; N, 4.94.

Crystallization of {(IMes)$_2$Cu}{Cu(Crp)$_2$}. A solution of (IMes)CuCl (0.200 g, 0.495 mmol) in THF (50 mL) was added to a solution of NaCrp (0.1317 g, 0.588 mmol) in THF (10 mL), and the resulting mixture was stirred overnight at room temperature. The mixture was then filtered through a pad of Celite and evaporated to dryness, giving a yellow solid. Crystals were obtained by diffusion of pentane vapors into a concentrated and filtered toluene solution at −36 °C. Yield: 0.228 g, 0.200 mmol, 40%. IR (solid, cm^{-1}): 1914 (ν_{CO}), 1822 (ν_{CO}), 1785 (ν_{CO}), 1013, 804, 738, 635. Anal. Calcd for $C_{58}H_{58}Cr_2Cu_2N_4O_6$: C, 61.20; H, 5.14; N, 4.92. Found: C, 61.87; H, 5.19; N, 4.97.

Solution Characterization Data for the Crp Derivatives Supported by IMes. ^{1}H NMR (500 MHz, C_6D_6): δ 6.72 (s, 4H, *m*-CH), 5.99 (s, 2H, NCH), 4.23 (s, Cp), 2.06 (s, 12H, *o*-CH_3), 2.04 (s, 6H, *p*-CH_3). $^{13}C\{^1H\}$ NMR (500 MHz, C_6D_6): δ 178.8 (NCCu), 139.3, 135.4, 134.8, 129.4, 121.4, 82.9 (Cp), 20.8, 17.4. Note: no peak corresponding to bound CO was located.

Preparation of {(IMes)$_2$Cu}{Cu(*Cc*)$_2$}. A solution of (IMes)CuCl (0.200 g, 0.494 mmol) in THF (50 mL) was added to a solution of NaCc (0.1149 g, 0.593 mmol) in THF (20 mL), and the resulting mixture was stirred overnight at 36 °C. The mixture was then filtered through a pad of Celite and evaporated to dryness, giving a light brown solid. Analytically pure crystals were obtained by diffusion of pentane vapors into a concentrated and filtered toluene solution at −36 °C. Yield: 0.2169 g, 0.233 mmol, 41%. ^{1}H NMR (500 MHz, C_6D_6): δ 6.74 (s, 4H, *m*-CH), 5.96 (s, 2H, NCH), 2.07 (s, 6H, *p*-CH_3), 1.96 (s, 12H, *o*-CH_3). $^{13}C\{^1H\}$ NMR (500 MHz, C_6D_6): δ 178.8 (NCCu), 139.6, 135.1, 134.5, 129.5, 121.4, 20.8, 17.3, 16.8. IR (solid, cm^{-1}): 2023 (ν_{CO}), 1906 (ν_{CO}), 1485, 1237, 1084, 1033, 851, 553, 533. Note: no peak corresponding to bound CO was located. Anal. Calcd for $C_{50}H_{48}Co_2Cu_2N_4O_8$: C, 55.71; H, 4.49; N, 5.20. Found: C, 56.20; H, 4.57; N, 5.10.

■ ASSOCIATED CONTENT

Ⓢ Supporting Information

Spectral characterization data, X-ray crystallographic data, and additional DFT output data are provided as Supporting Information. This material is available free of charge via the Internet at http://pubs.acs.org.

■ AUTHOR INFORMATION

Corresponding Author

*E-mail: npm@uic.edu.

Author Contributions

The manuscript was written through contributions of all authors. All authors have given approval to the final version of the manuscript.

Author Contributions

†These authors contributed equally.

Funding

Funding was provided by the UIC Department of Chemistry and College of Liberal Arts & Sciences, and by the National Science Foundation (No. CHE-1362294). Dr. Banerjee received support from the University Grants Commission (India) as a Raman Fellow for Postdoctoral Research for Indian Scholars in the United States.

Notes

The authors declare no competing financial interest.

■ ACKNOWLEDGMENTS

Computational resources were generously provided by Prof. Petr Kral. Dr. Dan McElheny assisted with NMR spectroscopy.

■ REFERENCES

(1) Selected references: (a) Jacobsen, E. N. *Acc. Chem. Res.* **2000**, *33*, 421−431. (b) Doyle, M. P. *J. Org. Chem.* **2006**, *71*, 9253−9260. (c) Reed, S. A.; White, M. C. *J. Am. Chem. Soc.* **2008**, *130* (11), 3316−3318. (d) Hirner, J. J.; Shi, Y.; Blum, S. A. *Acc. Chem. Res.* **2011**, *44*, 603−613. (e) Pérez-Temprano, M. H.; Casares, J. A.; Espinet, P. *Chem.—Eur. J.* **2012**, *18*, 1864−1884. (f) Kornecki, K. P.; Briones, J. F.; Boyarskikh, V.; Fullilove, F.; Autschbach, J.; Schrote, K. E.; Lancaster, K. M.; Davies, H. M. L.; Berry, J. F. *Science* **2013**, *342*, 351−354. (g) Powers, D. C.; Ritter, T. *Acc. Chem. Res.* **2012**, *45*, 840−850.

(2) Selected references: (a) Krogman, J. P.; Foxman, B. M.; Thomas, C. M. *J. Am. Chem. Soc.* **2011**, *133*, 14582−14585. (b) Rudd, P. A.; Planas, N.; Bill, E.; Gagliardi, L.; Lu, C. C. *Eur. J. Inorg. Chem.* **2013**, *2013*, 3898−3906. (c) Powers, T. M.; Betley, T. A. *J. Am. Chem. Soc.* **2013**, *135* (33), 12289−12296. (d) Chiarella, G. M.; Cotton, F. A.; Durivage, J. C.; Lichtenberger, D. L.; Murillo, C. A. *J. Am. Chem. Soc.* **2013**, *135*, 17889−17896. (e) Chernichenko, K.; Madarász, Á.; Pápai, I.; Nieger, M.; Leskelä, M.; Repo, T. *Nat. Chem.* **2013**, *5*, 718−723.

(3) Selected references: (a) Schmidt, J. A. R.; Lobkovsky, E. B.; Coates, G. W. *J. Am. Chem. Soc.* **2005**, *127*, 11426−11435. (b) Ahmed, S. M.; Poater, A.; Childers, M. I.; Widger, P. C. B.; LaPointe, A. M.; Lobkovsky, E. B.; Coates, G. W.; Cavallo, L. *J. Am. Chem. Soc.* **2013**, *135*, 18901−18911. (c) Zhou, W.; Marquard, S. L.; Bezpalko, M. W.; Foxman, B. M.; Thomas, C. M. *Organometallics* **2013**, *32*, 1766−1772. (d) Katcher, M. H.; Norrby, P.-O.; Doyle, A. G. *Organometallics* **2014**, *33*, 2121−2133. (e) Levin, M. D.; Toste, F. D. *Angew. Chem., Int. Ed.* **2014**, *53*, 6211−6215. (f) Anand, M.; Sunoj, R. B.; Schaefer, H. F., III. *J. Am. Chem. Soc.* **2014**, *136*, 5535−5538. (g) Sabater, S.; Mata, J. A.; Peris, E. *Nature Commun.* **2013**, *4*, 1−7.

(4) (a) Jayarathne, U.; Mazzacano, T. J.; Bagherzadeh, S.; Mankad, N. P. *Organometallics* **2013**, *32*, 3986−3992. (b) Karunananda, M. K.; Vazquez, F. X.; Alp, E. E.; Bi, W.; Chattopadhyay, S.; Shibata, T.; Mankad, N. P. *Dalton Trans.* **2014**, *43*, 13361−13671.

(5) Jayarathne, U.; Parmelee, S. R.; Mankad, N. P. *Inorg. Chem.* **2014**, *53*, 7730−7737.

(6) Mazzacano, T. J.; Mankad, N. P. *J. Am. Chem. Soc.* **2013**, *135*, 17258−17261.

(7) Other recent advances in C−H borylation by base metal catalysts: (a) Yan, G.; Jiang, Y.; Kuang, C.; Wang, S.; Liu, H.; Zhang, Y.; Wang, J. *Chem. Commun.* **2010**, *46*, 3170−3172. (b) Hatanaka, T.; Ohki, Y.; Tatsumi, K. *Chem.—Asian J.* **2010**, *5*, 1657−1666. (c) Obligacion, J. V.; Semproni, S. P.; Chirik, P. J. *J. Am. Chem. Soc.* **2014**, *136*, 4133−4136. (d) Fernández-Salas, J. A.; Manzini, S.; Piola, L.; Slawin, A. M. Z.; Nolan, S. P. *Chem. Commun.* **2014**, *50*, 6782−6784.

(8) Díez-González, S.; Nolan, S. *Synlett* **2007**, *2007*, 2158−2167.

(9) Mankad, N. P. *Synlett* **2014**, *25*, 1197−1201.

(10) Selected recent related studies: (a) Hicks, J.; Hoyer, C. E.; Moubaraki, B.; Manni, G. L.; Carter, E.; Murphy, D. M.; Murray, K. S.; Gagliardi, L.; Jones, C. *J. Am. Chem. Soc.* **2014**, *136*, 5283−5286. (b) Ma, M.; Sidiropoulos, A.; Ralte, L.; Stasch, A.; Jones, C. *Chem. Commun.* **2013**, *49*, 48−50. (c) Blake, M. P.; Kaltsoyannis, N.; Mountford, P. *Chem. Commun.* **2013**, *49*, 3315−3317. (d) Molon, M.; Gemel, C.; Seidel, R. W.; Jerabek, P.; Frenking, G.; Fischer, R. A. *Inorg. Chem.* **2013**, *52*, 7152−7160. (e) Bauer, J.; Braunschweig, H.; Dewhurst, R. D. *Chem. Rev. 112*, 4329−4346 and references therein.

(11) King, R. B. *Acc. Chem. Res.* **1970**, *3*, 417−427.

(12) (a) Dessy, R. E.; Pohl, R. L.; King, R. B. *J. Am. Chem. Soc.* **1966**, *88*, 5121−5124. (b) Lai, C. K.; Feighery, W. G.; Zhen, Y.; Atwood, J. D. *Inorg. Chem.* **1989**, *28*, 3929−3930.

(13) Fortman, G. C.; Slawin, A. M. Z.; Nolan, S. P. *Organometallics* **2010**, *29*, 3966−3972.

(14) (a) Ellis, D. D.; Couchman, S. M.; Jeffery, J. C.; Malget, J. M.; Stone, F. G. A. *Inorg. Chem.* **1999**, *38*, 2981−2988. (b) Enders, M.; Kohl, G.; Pritzkow, H. *Organometallics* **2002**, *21*, 1111−1117. (c) Shin, R. Y. C.; Teo, M. E.; Tan, G. K.; Koh, L. L.; Vittal, J. J.; Goh, L. Y.; Murray, K. S.; Moubaraki, B. *Organometallics* **2005**, *24*, 4265−4273. (d) Singh, A. K.; Levine, B. G.; Staples, R. J.; Odom, A. L. *Chem. Commun.* **2013**, *49*, 10799−10801.
(15) (a) Salm, R. J.; Ibers, J. A. *Inorg. Chem.* **1994**, *33*, 4216−4220. (b) Carlton, L.; Lindsell, W. E.; McCullough, K. J.; Preston, P. N. *J. Chem. Soc., Dalton Trans.* **1984**, 1693−1701. (c) Fischer, P. J.; Heerboth, A. P.; Herm, Z. R.; Kucera, B. E. *Organometallics* **2007**, *26*, 6669−6673. (d) Blagg, A.; Hutton, A. T.; Shaw, B. L.; Thornton-Pett, M. *Inorg. Chim. Acta* **1985**, *100*, L33−L34. (e) Carlton, L.; Lindsell, W. E.; McCullough, K. J.; Preston, P. N. *J. Chem. Soc., Chem. Commun.* **1983**, 216−218.
(16) (a) Apfel, J.; Klüfers, P.; Selle, A. *Z. Anorg. Allg. Chem.* **1995**, *621*, 323−330. (b) Achternbosch, M.; Apfel, J.; Fuchs, R.; Klüfers, P.; Selle, A. *Z. Anorg. Allg. Chem.* **1996**, *622*, 1365−1373. (c) O'Connor, C. J.; Freyberg, D. P.; Sinn, E. *Inorg. Chem.* **1979**, *18*, 1077−1088. (d) Hata, M.; Kautz, J. A.; Lu, X. L.; McGrath, T. D.; Stone, F. G. A. *Organometallics* **2004**, *23*, 3590−3602. (e) Kilbourn, B. T.; Blundell, T. L.; Powell, H. M. *Chem. Commun.* **1965**, 444−445.
(17) Kuppuswamy, S.; Bezpalko, M. W.; Powers, T. M.; Wilding, M. J. T.; Brozek, C. K.; Foxman, B. M.; Thomas, C. M. *Chem. Sci.* **2014**, *5*, 1617−1626.
(18) (a) Achternbosch, M.; Braun, H.; Fuchs, R.; Klüfers, P.; Selle, A.; Wilhelm, U. *Angew. Chem., Int. Ed. Engl.* **1990**, *29*, 783−785. (b) Darensbourg, D. J.; Chao, C. S.; Bischoff, C.; Reibenspies, J. H. *Inorg. Chem.* **1990**, *29*, 4637−4640. (c) Kautz, J. A.; McGrath, T. D.; Stone, F. G. A. *Polyhedron* **2003**, *22*, 109−118. (d) Doyle, G.; Eriksen, K. A. *Organometallics* **1985**, *4*, 877−881. (e) Fuchs, R.; Küfers, P. *J. Organomet. Chem.* **1992**, *424*, 353−370.
(19) Further information from spectroscopic and theoretical studies regarding the persistence of Cu-Fe bonding for (IPr)Cu-Fp in solution will be reported in a forthcoming manuscript.
(20) Ellis, J. E.; Flom, E. A. *J. Organomet. Chem.* **1975**, *99*, 263−268.
(21) Kalz, K. F.; Kindermann, N.; Xiang, S.-Q.; Kronz, A.; Lange, A.; Meyer, F. *Organometallics* **2014**, *33*, 1475−1479.
(22) Cotton, F. A.; Daniels, L. M.; Murillo, C. A.; Zhou, H.-C. *Inorg. Chim. Acta* **2000**, *300*−*302*, 319−327.
(23) Covalent radii values: Pauling, L. *J. Am. Chem. Soc.* **1947**, *69*, 542−553.
(24) Sum of the van der Waals radii of Cu and C is ∼4.2 Å; see: Alvarez, S. *Dalton Trans.* **2013**, *42*, 8617−8636.
(25) Curtis, M. D.; Han, K. R.; Butler, W. M. *Inorg. Chem.* **1980**, *19*, 2096−2101.
(26) This corrects our previous assertion that the (IPr)Cu−Fp structure features only one close Cu···CO contact rather than two.
(27) Caytan, E.; Roland, S. *Organometallics* **2014**, *33*, 2115−2118.
(28) Darensbourg, D. J.; Chao, C. S.; Reibenspies, J. H.; Bischoff, C. J. *Inorg. Chem.* **1990**, *29*, 2153−2157.
(29) Doyle, G.; Eriksen, K. A.; Van Engen, D. *J. Am. Chem. Soc.* **1985**, *107*, 7914−7920.
(30) Sheldrick, G. M. *Acta Crystallogr., Sect. A: Found. Crystallogr.* **2008**, *A64*, 112.
(31) Müller, P. *Cryst. Rev.* **2009**, *15*, 57.
(32) Behrens, U.; Edelmann, F. *J. Organomet. Chem.* **1984**, *263*, 179−182.
(33) (a) Jafarpour, L.; Stevens, E. D.; Nolan, S. P. *J. Organomet. Chem.* **2000**, *606*, 49−54. (b) Arduengo, A. J., III; Krafczyk, R.; Schmutzler, R.; Craig, H. A.; Goerlich, J. R.; Marshall, W. J.; Unverzagt, M. *Tetrahedron* **1999**, *55*, 14523−14534. (c) Hintermann, L. *Beilstein J. Org. Chem.* **2007**, *3*, 22.
(34) (a) Santoro, O.; Collado, A.; Slawin, A. M. Z.; Nolan, S. P.; Cazin, C. S. J. *J. Chem. Soc., Chem. Commun.* **2013**, *49*, 10483−10485. (b) Kaur, H.; Zinn, F. K.; Stevens, E. D.; Nolan, S. P. *Organometallics* **2004**, *23*, 1157−1160.
(35) Gaussian 09, Revision B.01, Frisch, M. J.; Trucks, G. W.; Schlegel, H. B.; Scuseria, G. E.; Robb, M. A.; Cheeseman, J. R.; Scalmani, G.; Barone, V.; Mennucci, B.; Petersson, G. A.; Nakatsuji, H.; Caricato, M.; Li, X.; Hratchian, H. P.; Izmaylov, A. F.; Bloino, J.; Zheng, G.; Sonnenberg, J. L.; Hada, M.; Ehara, M.; Toyota, K.; Fukuda, R.; Hasegawa, J.; Ishida, M.; Nakajima, T.; Honda, Y.; Kitao, O.; Nakai, H.; Vreven, T.; Montgomery, J. A.; , Jr., Peralta, J. E.; Ogliaro, F.; Bearpark, M.; Heyd, J. J.; Brothers, E.; Kudin, K. N.; Staroverov, V. N.; Keith, T.; Kobayashi, R.; Normand, J.; Raghavachari, K.; Rendell, A.; Burant, J. C.; Iyengar, S. S.; Tomasi, J.; Cossi, M.; Rega, N.; Millam, J. M.; Klene, M.; Knox, J. E.; Cross, J. B.; Bakken, V.; Adamo, C.; Jaramillo, J.; Gomperts, R.; Stratmann, R. E.; Yazyev, O.; Austin, A. J.; Cammi, R.; Pomelli, C.; Ochterski, J. W.; Martin, R. L.; Morokuma, K.; Zakrzewski, V. G.; Voth, G. A.; Salvador, P.; Dannenberg, J. J.; Dapprich, S.; Daniels, A. D.; Farkas, O.; Foresman, J. B.; Ortiz, J. V.; Cioslowski, J.; Fox, D. J. *Gaussian 09, Revision B.01*; Gaussian, Inc., Wallingford, CT, 2010.
(36) Becke, A. D. *Phys. Rev. A* **1988**, *38*, 3098−3100.
(37) Perdew, J. P. *Phys. Rev. B* **1986**, *33*, 8822−8824.
(38) (a) Hay, P. J.; Wadt, W. R. *J. Chem. Phys.* **1985**, *82*, 299. (b) Roy, L. E.; Hay, P. J.; Martin, R. L. *J. Chem. Theory Comput.* **2008**, *4*, 1029. (c) Ehlers, A. W.; Bohme, M.; Dapprich, S.; Gobbi, A.; Hollwarth, A.; Jonas, V.; Kohler, K. F.; Stegmann, R.; Veldkamp, A.; Frenking, G. *Chem. Phys. Lett.* **1993**, *208*, 111.
(39) (a) Hay, P. J.; Wadt, W. R. *J. Chem. Phys.* **1985**, *82*, 270. (b) Hay, P. J.; Wadt, W. R. *J. Chem. Phys.* **1985**, *82*, 284.
(40) Glendening, E. D.; Reed, A. E.; Carpenter, J. E.; Weinhold, F. *NBO, Version 3.1*.
(41) Angelici, R. J.; Chin, T. T.; Hoyano, J. K.; Legzdins, P.; Malito, J. T.; Arnold, T.; Swanson, B. I. *Inorg. Synth.* **1990**, *28*, 196−198.